High doping effects on *in-situ* Ohmic contacts to n-InAs

Ashish Baraskar[1], Vibhor Jain[1], Mark A. Wistey[3], Uttam Singisetti[1], Yong Ju Lee[4], Brian Thibeault[1], Arthur Gossard[1,2] and Mark J. W. Rodwell[1]

[1]ECE and [2]Materials Departments, University of California, Santa Barbara, CA, USA
[3]Electrical Engineering, University of Notre Dame, IN, USA
[4]Intel Corporation, Technology Manufacturing Group, Santa Clara, CA, USA

ABSTRACT

We present the effect of active carrier concentration on the specific contact resistivity (ρ_c) of *in-situ* molybdenum (Mo) Ohmic contacts to *n*-type InAs. It is observed that, although the Fermi level pins in the conduction band for InAs, the contact resistivity decreases with the increase in InAs active carrier concentration. The lowest ρ_c obtained through transmission line model measurements was $(0.6 \pm 0.4) \times 10^{-8}$ Ω-cm^2 for samples with 8.2×10^{19} cm^{-3} active carrier concentration. The contacts were found to remain stable on annealing at 250 ^{o}C for 1 hour.

I. INTRODUCTION

Ultra-low resistance metal-semiconductor contacts are fundamental to the continued scaling of transistors towards THz bandwidths. Geometric scaling laws show that doubling transistor bandwidths requires a four-fold reduction in specific contact resistivity (ρ_c) (1, 2). $\rho_c <$ 1×10^{-8} Ω-cm^2 is necessary in III-V HBTs and FETs for having simultaneous 1.5 THz f_t and f_{max} (1, 2). Moreover, high temperature operation and high current densities in modern electronic devices require the contact to be thermally stable (3).

Fabrication of Ohmic contacts using ex-situ techniques requires a significant attention to removal of semiconductor oxides and contaminants (4). Obtaining repeatable contacts through *ex-situ* techniques requires good process control; ρ_c can be highly sensitive to surface preparation and to the time interval between the surface preparation and contact metal deposition. Contacts formed through *in-situ* techniques are repeatable and result in ultra-low contact resistivities (5). *In-situ* technique involves contact metal deposition immediately after semiconductor growth without exposing the semiconductor surface to air preventing surface contamination and oxidation.

Apart from surface preparation, the interface conduction band barrier potential, determined either by Fermi level pinning or by work functions, also plays a crucial role in determining the contact resistance. For InAs, the Fermi level is pinned in the conduction band (6, 7, 8) which makes it a potential candidate to be used as the contact layer for metal-semiconductor contacts. *Ex-situ*, annealed, contacts to InAs with 2×10^{19} cm^{-3} active carrier concentration have shown to result in $\rho_c = 2\times10^{-8}$ Ω-cm^2 (9). Ohmic contacts to GaAs and $In_{0.53}Ga_{0.47}As$ using an InAs cap layer have been studied extensively (9, 10, 11). The contact resistance to GaAs (using an InAs cap layer) decreases on increasing the GaAs active carrier concentration because of the increased tunneling across the InAs/GaAs heterojunction (10). The active carrier concentration in InAs was kept constant in these samples. However, there have been no reports on the effect of InAs active carrier concentration on ρ_c. Here we present the dependence of ρ_c on InAs active carrier concentration. We report a ρ_c of $(0.6\pm0.4)\times10^{-8}$ Ω-cm^2 for non-alloyed, in-situ, refractory molybdenum (Mo) contacts to n-type InAs with 8.2×10^{19} cm^{-3} active carrier concentration.

II. EXPERIMENTAL DETAILS

The semiconductor epilayers were grown by a Gen II solid source MBE system. A 150 nm undoped $In_{0.52}Al_{0.48}As$ layer was grown on a semi-insulating InP (100) substrate, followed by 100 nm of silicon (Si) doped InAs. The samples were grown at 400 °C substrate temperature with the Si cell temperature varying from 1190 ^{o}C to 1390 ^{o}C. After the InAs growth, the wafer was cooled and transferred under UHV to an electron beam evaporation chamber, where 20 nm of molybdenum (Mo) was deposited on half the wafer through a shadow mask (5). The active carrier concentration, mobility and sheet resistance were obtained from Hall measurements by placing indium contacts on samples taken from the half of the wafer not coated with Mo. The portion of the wafer coated with Mo was processed into transmission line model (TLM) structures for contact resistance measurement.

To extract the specific contact resistivity, the samples were processed into TLM structures (12). For the TLM structures (Fig. 1), Ti (20 nm) /Au (500 nm) /Ni (50 nm) contact pads were patterned using optical photolithography and lifted-off after an e-beam deposition. The Au layer is 500 nm thick to reduce interconnect resistance. Mo was then dry etched in an SF_6/Ar plasma using Ni as an etch mask. The TLM structures were then isolated using mesas formed by photolithography and a subsequent wet etch. A schematic of the TLM pattern is shown in Fig. 2.

50 nm ex-situ Ni
500 nm ex-situ Au
20 nm ex-situ Ti
20 nm in-situ Mo
100 nm InAs: Si (n-type)
150 nm $In_{0.52}Al_{0.48}As$: NID buffer
Semi-insulating InP: Substrate

Fig. 1: Cross-section schematic of the metal-semiconductor contact layer structure used for TLM measurements.

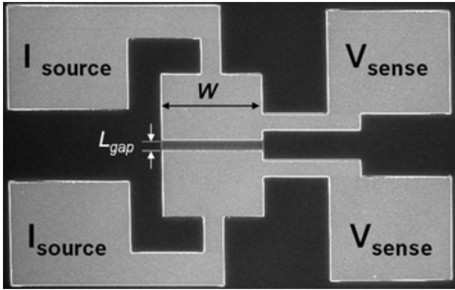

Fig. 2: Schematic of the TLM pattern used for the contact resistivity measurement. Separate pads were used for current biasing and voltage measurement

Resistances were measured using a four-point (Kelvin) probe technique on an Agilent 4155C semiconductor parameter analyzer (5). In the Kelvin probing structure (Fig. 2), the observed resistance,

$$R_{measured} = 2\rho_c / WL_T + \rho_s L_{gap} / W + R_{metal}$$

contains a small contribution R_{metal} from the sheet resistivity (ρ_m / T_m) of the contact metal. Here ρ_c is the metal-semiconductor contact resistivity, ρ_s the semiconductor sheet resistivity, $L_T = \sqrt{\rho_c / \rho_s}$ the transfer length, ρ_m the bulk metal resistivity and T_m the contact metal thickness. The dimensions W and L_{gap} are defined in Fig. 2. R_{metal} is determined from separate measurements of ρ_m / T_m and from numerical finite-element analysis of the contact geometry. For the narrow width (W=10 µm) test structures, R_{metal} changes the contact resistivity data by less than 5 %. Note that the TLM geometry used here (Fig. 2) differs from that used in (5), and the associated R_{metal} term reduced by over 4:1 for W=10 µm.

The sheet resistance of the semiconductor between the contacts does not change after being exposed to SF_6/Ar plasma etch for removing Mo (5). This validates the extraction of the contact resistivity (ρ_c) from the observed lateral access resistivity (ρ_H) and semiconductor sheet resistivity (ρ_s).

III. RESULTS AND DISCUSSION

Fig. 3 shows the variation of active carrier concentration and mobility with Si atomic concentration. For Si atomic concentration greater than 2×10^{20} cm^{-3}, the active carrier concentration was found to saturate because of the auto-compensation behavior of Si at greater atomic concentrations (13). The highest active carrier concentration obtained was 1.2×10^{20} cm^{-3} for a total Si atom concentration of 3.5×10^{20} cm^{-3}. InAs layers grown with Si atom concentration greater than 3.5×10^{20} cm^{-3} resulted in rough and hazy surfaces, probably due to excessive Si incorporation in the layers (13).

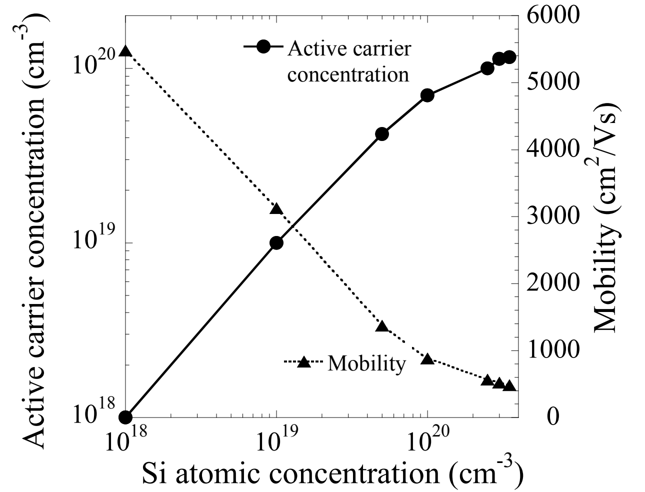

Fig. 3: Variation of active carrier concentration and mobility with Si atomic concentration.

Fig. 4 shows ρ_c as a function of active carrier concentration. For active carrier concentration below 8.2×10^{19} cm^{-3}, ρ_c decreases with increase in the active carrier concentration and saturates for an active carrier concentration greater than 8.2×10^{19} cm^{-3}. This indicates that, although the Fermi level pins in the conduction band for InAs, an active carrier concentration greater than ~ 4×10^{19} cm^{-3} is required to obtain ρ_c less than 1×10^{-8} Ω-cm^2. The lowest ρ_c extracted from the TLM measurements was $(0.6\pm0.4)\times10^{-8}$ Ω-cm^2 for the sample with an active carrier concentration of 8.2×10^{19} cm^{-3}. For this sample, the variation of TLM test structure resistance with contact separation is shown in Fig. 5. Note that after

correcting for the effect of TLM test structure interconnect resistance on measurements (5), we had earlier obtained ρ_c = (1.4±0.5)×10^{-8} Ω-cm^2 for in-situ Mo contacts to a composite layer of 5 nm of n-type InAs on 95 nm of InGaAs (14). For this sample, the active carrier concentration in the InAs layer was 3 ×10^{19} cm^{-3} (calibrated on separate samples). As shown in Fig. 4, ρ_c reported for InAs (5 nm) /InGaAs (95 nm) sample of ref. (14) is greater than expected from the current data because the observed resistivity includes Mo/InAs and InAs/InGaAs interfaces in series. Also shown in Fig. 4 is the ρ_c obtained with *ex-situ*, annealed, contacts to InAs (9), which is greater than for *in-situ* contacts.

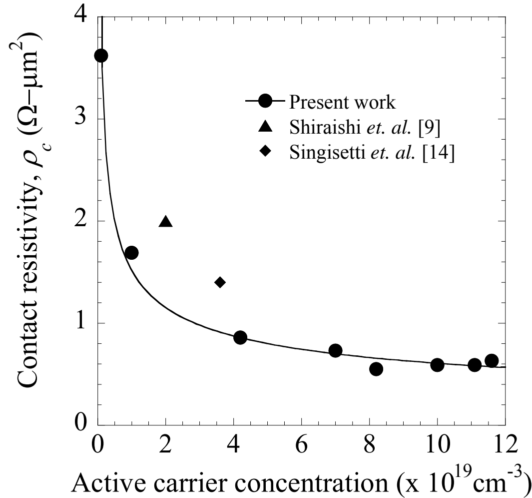

Fig. 4: Variation of specific contact resistivity with active carrier concentration.

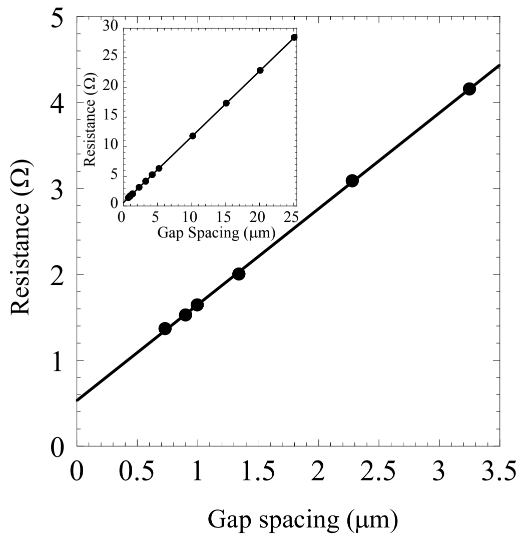

Fig. 5: Measured TLM resistance as a function of pad spacing for the sample with ρ_c = (0.6±0.4)×10^{-8} Ω-cm^2. The inset plots measured TLM resistance vs. pad spacing ranging from 0.8 µm to 25 µm.

For the sample with ρ_c = (0.6±0.4)×10^{-8} Ω-cm^2, the transfer length was 260 nm, 2.6:1 larger than the N+ layer thickness; hence resistance analysis assuming one-dimensional current flow is appropriate. Hall measurements on the same sample with lowest contact resistivity indicate 568 cm^2/Vs mobility, and 10.5 Ω sheet resistivity. The sheet resistivity determined from TLM measurements was 11 Ω, correlating closely to the sheet resistivity obtained with Hall measurements.

To study the thermal stability of the contacts, the processed samples were annealed under nitrogen atmosphere at 250 ^{o}C for 1 hour, a thermal cycle representative of the curing cycle of the benzocyclobutene (BCB) passivation and interconnect dielectric used in many III-V IC processes (15). The contacts were found to remain Ohmic and the observed variation in the contact resistivity was less than the margin of error in the measurement.

IV. CONCLUSIONS

We present the dependence of ρ_c on active carrier concentration for *in-situ,* thermally stable, Ohmic contacts to InAs. We show that, although the Fermi level pins in the conduction band for InAs, ρ_c decreases with increased active carrier concentration for active carrier concentrations below 8.2×10^{19} cm^{-3}. ρ_c was found to saturate for active carrier concentrations above 8.2×10^{19} cm^{-3} and the lowest ρ_c obtained was (0.6±0.4)×10^{-8} Ω-cm^2. Our results indicate that active carrier concentrations in excess of ~ 4×10^{19} cm^{-3} are required to obtain ρ_c less than 1×10^{-8} Ω-cm^2. These results indicate the effectiveness of InAs in forming ultra-low resistance Ohmic contacts; application in contacts to layers within III-V devices requires further characterization of the heterojunction interface resistance between InAs and the contacting layer.

ACKNOWLEDGMENTS

This work was supported by the ONR and by the DARPA THETA (program number G9U571158). A portion of this work was done in the UCSB nanofabrication facility, part of the NSF funded NNIN network.

REFERENCES

1. M. J. W. Rodwell, M. L. Le, B. Brar, *IEEE Proceedings*, **96**, 2, 271–286 (2008).
2. M. J. W. Rodwell et al., Proceedings, *IEEE Compound Semiconductor Integrated Circuit Symposium*, 2008.
3. Yoshino K. Fukai, Kenji Kurishima, Norihide Kashio, Minoru Ida, Shoji Yamahata, Takatomo Enoki, *Microelectronics Reliability*, **49**, 357–364 (2009).
4. Vibhor Jain, Ashish K. Baraskar, Mark A. Wistey, Uttam Singisetti, Zach Griffith, Evan Lobisser, Brian

J. Thibeault, Arthur C. Gossard, and Mark. J. W. Rodwell, *21th IEEE International Conference on Indium Phosphide and Related Materials*, 10–14 May 2009, pp. 358–361.

5. Ashish Baraskar, Mark A. Wistey, Vibhor Jain, Uttam Singisetti, Greg Burek, Brian Thibeault, Yong Ju Lee, Arthur Gossard and Mark Rodwell, *J. Vac. Sci. Tech. B*, **27**, 2036 (2009).
6. C. A. Mead and W. G. Spitzer, *Phys. Rev*., **134**, A713 (1964).
7. L. J. Brillson, M. L. Slade, R. E. Viturro, M. K. Kelly, N. Tache, G. Margaritondo, J. M. Woodall, P. D. Kirchner, G. D. Pettit, and S. L. Wright, *Appl. Phys. Lett.*, **48**, 1458 (1986).
8. S. Bhargava, H. R. Blank, V. Narayanamurti, and H. Kroemer, *Appl. Phys. Lett*., **70**, 759 (1997).
9. Y. Shiraishi, N. Furuhata, and A. Okamoto, *J. Appl. Phys.,* **76**, 5099 (1994).
10. S.L. Wright, R. F. Marks, S. Tiwari, T. N. Jackson, and H. Baratte, *Appl. Phys. Lett.,* **49**, 1545 (1986).
11. C. K. Peng, J. Chen, J. Chyi, and H. Morkoc, *J. Appl. Phys.*, **64**, 1, 429–431 (1988).
12. H. H. Berger, *Solid-State Electron*., **15**, 145 (1972)
13. Y. G. Chai, R. Chow, and C. E. C. Wood, *Appl. Phys. Lett.*, **39**, 800 (1981).
14. U. Singisetti, M. A. Wistey, J. D. Zimmerman, B. J. Thibeault, M. J. W. Rodwell, A. C. Gossard, and S. R. Bank, *Appl. Phys. Lett.,* **93**, 183502 (2008).
15. Zach Griffith, Young Min Kim, Mattias Dahlström, Arthur C. Gossard, and Mark J. W. Rodwell*, IEEE Elec. Dev. Lett.*, **25**, 10 (2004).